Desalination and Water Treatment
www.deswater.com

doi: 10.5004/dwt.2019.24468

170 (2019) 128–137
December

Fixed-bed column study for the removal of hexavalent chromium ions from aqueous solutions via pyrolysis of rice husk

Sobhy M. Yakout[a,b,*], Mohamed R. Hassan[c], Hoda A. Omar[c]

[a]*Department of Biochemistry, College of Science, King Saud University, P.O. Box: 2455, Riyadh 11451, Saudi Arabia, Tel. +00966558448693; Fax: +96614675931; email: syakout@ksu.edu.sa*
[b]*Department of Analytical Chemistry and Control, Hot Laboratories and Waste Management Center, Atomic Energy Authority, Cairo 13759, Egypt*
[c]*Nuclear Research Center, Atomic Energy Authority, P.O. Box: 13759, Inshas, Cairo, Egypt, Tel. +00201008537038; email: muhmmed_refait@yahoo.com (M.R. Hassan), Tel. +00201005546429; email: hodaatom@yahoo.com (H.A. Omar)*

Received 10 November 2018; Accepted 28 May 2019

ABSTRACT

The elimination of hexavalent chromium ions from laden aqueous solution using rice husk ash (RHA) as a biosorbent from rice husk (RH) was investigated based on different experimental parameters of the continual fixed-bed column system. Fourier transform infrared spectrometry and scanning electron microscopy (SEM) were used to characterize RHA and RH. The result of varied parameters such as bed height (2.5, 4.3 and 5.8 cm), influent flow rate (5, 10 and 15 mL/min) and initial hexavalent chromium concentrations (50, 100 and 150 mg/L) seemed to be researched. The exhaustion period elevated with an increasing in bed height but reduced with a decreasing of both flow rate and initial concentration. The Thomas, Yoon–Nelson, Adams–Bohart mathematical models were successfully utilized to the biosorption within different experimental parameters conditions to predict the breakthrough curves and to assess the model experimental parameters of the fixed-bed column, which are valuable for process design. Yoon–Nelson model was found suitable for describing the experimental data than Thomas and Adams–Bohart models. The performance of RHA column investigation states the value of the good biosorption capacity for elimination of hexavalent chromium from laden aqueous solution.

Keywords: Hexavalent chromium; Rice husk ash; Adsorption; Fixed-bed column

1. Introduction

Several poisonous heavy metal ions released via various manufacturing industries are one of the major causes of water pollution. Heavy metal residues within polluted habitats may perhaps accumulate throughout microorganisms, aquatic flora and fauna, which in turn may possibly start the human food chain with serious disorders [1–4]. Chromium occurs in nature as $Cr^{3+}$and Cr^{6+} [5]. The hexavalent chromium is mostly present in the form of dichromate and chromate ions are much more poisonous than Cr^{3+} [6]. Chromium waste is produced from several manufacturing processes, for example, electroplating, steel manufacture, leather dyeing, wood protection, textile coloring, paint, pigments, petroleum purifying procedures and so on [7]. According to the World Health Organization, the levels of hexavalent chromium in drinking water, internal surface water, and manufacturing wastewater are 0.05, 0.1 and 0.25 mg/L, respectively [8]. Therefore, it is essential to reduce hexavalent chromium from water/wastewater, and it is vital that the discharges should be maintained before emitting hexavalent chromium into marine environments.

* Corresponding author.

The technology of adsorption was considered to be one of the most widespread technologies for metals ions removal from water pollution control because of low cost, ease of process and simplicity of design [9,10]. The application of agro-wastes as biosorbents is presently obtaining wide care because of cheap owing to relatively high of percentage carbon content, its availability and porous structure. Several researchers have described the purpose of a continuous column packed with various kinds of biosorbents for the management of wastewater [11]. The use of the inexpensive and readily presented biosorbent was described to establish their efficacy on eliminating the metal from laden aqueous solution.

Rice husk ash (RHA) is prepared by pyrolysis of rice husk, which is a low-cost agrarian waste was obtained from the mills of rice after rice separation. RHA has good biosorption and has been utilized for the elimination of heavy metals [12–14], different dyes [15,16], palmytic acid [17] and other compounds as chlorinated hydrocarbons [18].

Nakkeeran et al. [19] have reported that the column biosorption investigations were operated to test the ability of *Strychnos nux-vomica* tree fruit shell towards Cr(VI) removal from simulated aqueous solution. Effect of different factors such as bed height, flow rate inside the column and initial concentration of Cr(VI) in aqueous solution for removal of Cr(VI) were investigated. The results showed that Cr(VI) adsorption capacity (mg/g) marked up with the increase in bed height; decreased with raise in flow rate and initial concentrations of Cr(VI).

Saranya et al. [20] had published that the Cr(VI) removal was studied with *Artocarpus heterophyllus* peel as a biosorbent in batch and continuous mode. Continuous column studies at different feed flow rates, initial feed Cr(VI) concentration, and column bed height were optimized using simulated tannery effluents. Results of the present study depicted that *Artocarpus heterophyllus* peel biosorbent can be utilized for the removal of Cr(VI) from simulated and real effluents.

Rangabhashiyam et al. [21] described the removal of Cr(VI) from aqueous solution by a novel *Swietenia mahogani* fruit shell physically activated carbon (SMFS-PAC) was examined in a packed bed column study. The effects of significant parameters such as feed flow rate, bed height, and initial Cr(VI) concentration were studied. Column data obtained at different conditions were described using the Thomas, bed depth service time (BDST), Adams–Bohart, and Yoon–Nelson model in order to predict the breakthrough curves and to evaluate the model parameters of the packed bed column studies data. Among the models used, Thomas, BDST, and Yoon–Nelson model, respectively, fitted to the experimental data very well. The SMFS-PAC column study states the value of the good adsorption capacity for the removal of Cr(VI) from aqueous solution.

The present study was focused on the removal of hexavalent chromium from aqueous solutions in a fixed-bed column using RHA. The hexavalent chromium uptake capacity of RHA was investigated as a function of various operating parameters such as flow rate, initial hexavalent chromium concentration, and bed height. The experimental data were utilized in three different kinetic models to find out the best fit.

2. Materials and methods

2.1. Adsorbate

A stock solution of hexavalent chromium (500 mg/L) was made by dissolving 1.4143 g of $K_2Cr_2O_7$ in double distilled de-ionized water. All of the chemical substances are of analytical reagent grade.

2.2. Preparation of the RHA

Rice husk (RH) was chosen as a predecessor material for the production of RHA. A sample of rice husk (RH) was extracted from a local rice generator. The RH sample was pyrolysed in a muffle furnace at 700°C for 1 h in the privation of air. The prepared carbon pyrolysis sample was placed into DW and then isolated by filtering. The filtrate sample has soaked up again in an oven at 90°C for 1 d and finally, the particle of carbon was sieved to obtain particles size between 1 and 2 mm which was utilized for all the trials.

2.3. Column studies

Experiments of the column were carried for biosorption of hexavalent chromium at optimum pH 2.5, bed height, flow rate and initial hexavalent chromium concentration from a previous study [22–25]. The fixed-bed column was made of glass with a height of 20 cm and an internal diameter of 1 cm. To analyse the influence of bed height, column was packed with either 1.5, 3 or 4.5 g of RHA to get a particular bed height of the sorbent (2.5, 4.3 and 5.8 cm of bed height) at 30°C and pH 2.5, keeping flow rate and initial hexavalent chromium concentration constant at 5 mL/min and 100 mg/L, respectively. To analyze the effect of concentration, hexavalent chromium solution of known concentrations either 50, 100 or 150 mg/L at 30°C and pH 2.5, keeping bed height and flow rate constant at 2.5 cm and 5 mL/min, respectively. To analyze the effect of flow rate, hexavalent chromium solution was flowing throughout the column at the desired flow rate either 5, 10 or 15 mL/min at 30°C and pH 2.5, keeping bed height and constant at 2.5 cm and 100 mg/L. The samples of effluent were collected at regular periods to measure the concentration of hexavalent chromium in the solutions. The flow in the fixed-bed column was carried out continuously until the effluent concentration of hexavalent chromium reached the same as the concentration of influent [26,27].

2.4. Analytical techniques

The hexavalent chromium was valued established on colorimetric technique via UV spectrophotometer (Shimadzu model 160A double-beam, Shimadzu Co., Japan) at 540 nm wavelength using 1,5-diphenyl carbazide technique when the pink complex created. This technique can verify hexavalent chromium in the range from 0.10 to 1.0 mg/L [11].

2.5. Column data analysis

The breakthrough curve is an important indicator to explain the adsorption performance of a column. Fig. 1 illustrates a perfect breakthrough curve, where the adsorption

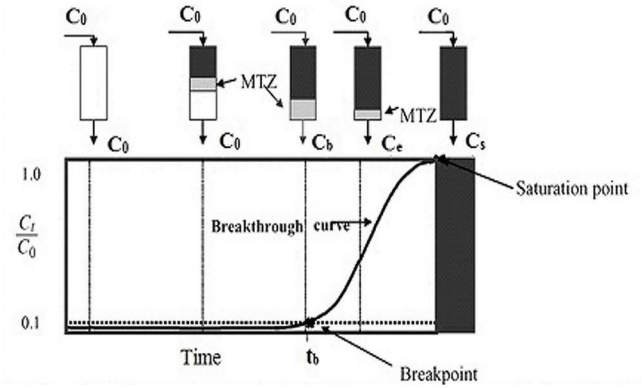

Fig. 1. Representation of a typical breakthrough curve.

happens on the surface of the bed, which is called the mass transfer zone. At the point when the volume of the liquid starts to move through the column, the mass transfer zone varies from 0% to 100% of the feed concentration. From a practical point of view, the saturation time, t_s, is established when metal ions concentration in the effluent reaches 95% of the feed concentration. Breakthrough time, t_b, is established when the metal ions concentration in the effluent reaches a determined value. The breakthrough curve is expressed as a function of the ratio of the hexavalent chromium concentration (mg/L) of the effluent to the hexavalent chromium ions concentration (mg/L) of the inlet, (C_t/C_0), to the time (min) or volume (mL) after the flow started. The volume of the effluent, V_{eff} (mL), was computed according to the following equation [28,29].

$$V_{eff} = Qt_{total} \tag{1}$$

Here Q (the volumetric flow rate in mL/min), t_{total} (the total flow time in min). The value of the total mass of hexavalent chromium sorbed, q_{total} (mg), can be computed from the area under the breakthrough curve [30]:

$$q_{total} = \frac{Q}{1{,}000}\int_{t=0}^{t=total} C_{ad}\,dt \tag{2}$$

Here C_{ad} (the concentration of hexavalent chromium removal in mg/L). Equilibrium metal uptake may be the optimum capacity of the column, q_{eq} (mg/g), in the column is computed as the next:

$$q_{eq} = \frac{q_{total}}{D} \tag{3}$$

Here D (the dry weight of sorbent in the column in g). The total amount of hexavalent chromium entering column (m_{total}) is computed according to the following equation [31]:

$$m_{total} = \frac{C_0 Q\, t_{total}}{1{,}000} \tag{4}$$

And the removal percentage of hexavalent chromium can be got from Eq. (5) as follows:

$$Y(\%) = \frac{q_{total}}{m_{total}} \times 100 \tag{5}$$

3. Results and discussion

3.1. Characterization of prepared RHA biosorbent

The physicochemical characterization of biosorbent tests arranged has been done; the surface of RHA biosorbent arranged has been examined utilizing SEM (scanning electron microscope), to recognize the functional group in charge of adsorption Fourier transform infrared spectroscopy (FTIR) examination was completed. The point zero charge pH(pzc) of RHA biosorbent, that is, the pH for which the surface charge is zero, is determined to utilize a method similar to that illustrated earlier [32]. Assuming that production cost advantages exist by using rice husk based carbons instead of currently available commercial activated carbons, there is potential to create new demand for the husk-derived adsorbents, thus stimulating the market for them and widening their usage further. Egypt has abundantly available agricultural waste, such as rice husk, which has very little economic value and in fact, often creates a serious problem of disposal for local environment.

3.1.1. Scanning electron microscopy

The SEM micrographs for RH and RHA with magnification at 1,000 are shown in Fig. 2. SEM of RH demonstrates surface geology with no pore. SEM picture of RHA demonstrates a porous structure in nature.

3.1.2. Fourier transforms infrared spectroscopy

Infrared spectroscopy gives us useful information about surface functional groups and the chemical structure of the samples. Fig. 3 exhibits the FTIR spectra of the RH and RHA. The characterization of rice husks by broadband between 3,700 and 3,000 cm^{-1}. The intense absorption band observed at 3,345 cm^{-1} can be assigned either to O–H stretching vibrations in the water molecules, OH groups presented in lignin, cellulose, and hemicellulose or to bonded by hydrogen bonds [33]. The band observed near 1,654 cm^{-1} is assigned to water molecules vibrations [34]. The position and asymmetry of these bands at lower wave numbers, indicating the presence of strong hydrogen bonds. It presents signals at 2,925 cm^{-1} which assigned to the symmetric and asymmetric stretching vibrations of CH_3 or CH_2 group. The appearance of a peak at 1,716 cm^{-1} was related to the stretching vibrations of C=O from the aldehyde groups of hemicellulose. The triplet in the IR spectra of rice husk recorded in the region 1,200–1,000 cm^{-1} was considered to result from the superposition of vibrations of the C–OH bond and Si–O bond in the siloxane (Si–O–Si) groups.

The intense band at 1,100 cm^{-1} corresponds to the stretching vibrations of silicon–oxygen tetrahedrons. The high intensity of this peak was probably caused by superposition of the stretching vibrations of the C–OH bond in the interval

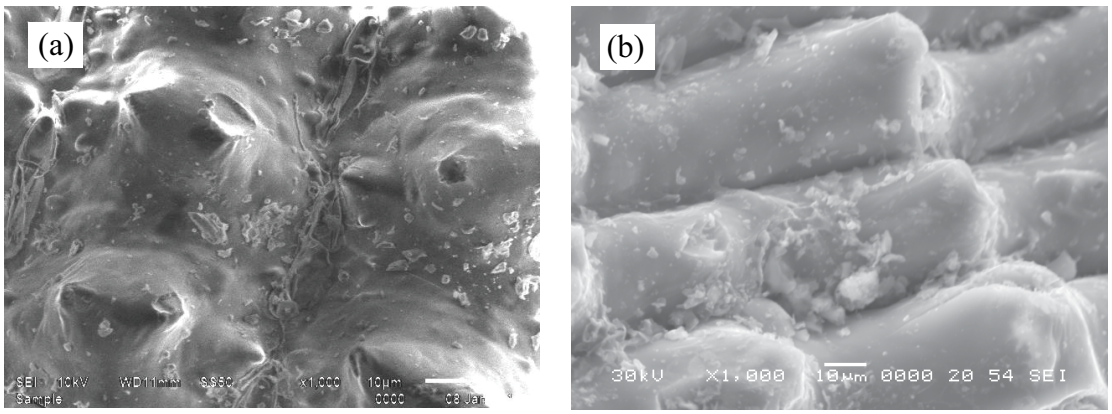

Fig. 2. SEM of RH (a), RHA (b).

1,200–1,000 cm^{-1} and the stretching vibrations of the Si–O bond. The observed weak bands at 868 and 800 cm^{-1} ascribed to the symmetric and antisymmetric vibrations of the Si–O bonds in the silicon–oxygen network. The absorbance at 455 cm^{-1} corresponded to bending vibration of siloxane bonds.

For FTIR spectra of RHA, Two bands at around 3,401 and 1,080 cm^{-1} are assigned to the –OH vibrations and hence indicating the presence of surface hydroxyl groups and chemisorbed water. The band at 3,401 cm^{-1} is attributed to both free and hydrogen bonded O–H groups. The bands observed near 1,078 and 795 cm^{-1} are in correspondence to O-Si-O stretching and that at near 458 cm^{-1} to bending. [35].

3.1.3. Determine the point zero charge pH(pzc)

pH zero point charge (pHzpc) of RHS was determined by shaking 0.1 g of the RHS with 20 mL of 0.01 mol/L of KNO_3 solutions are sited in various locked conical flasks pH value is adjusted between 1 and 10 by adding HCl (0.1 M) or NaOH (0.1 M) and kept overnight under stirring at a temperature 30°C. The pH(zpc) of RHS is the point where the curve of final pH (pH_f) against initial pH (pH_o) crosses the line at (pH_f) equal (pH_o).

RHS pH at the point of zero charge (pHpzc) can also influence the ionic state of the functional group on the RHS surface. From the analysis, the estimate of pHpzc of RHS was determined to be 8 as shown in Fig. 4.

Below this pHpzc value, the surface gains a positive charge and above it, the surface is given with a negative charge and the surface is neutral at same pHpzc value. Hence, below this pHpzc value, the predominating charge on the RHS biosorbent surface is positive which entices the negatively charged chromate ions and hence, the removal percentage is more. But above this pHpzc value, RHS biosorbent surface, as well as hexavalent chromium ions species, has a negative

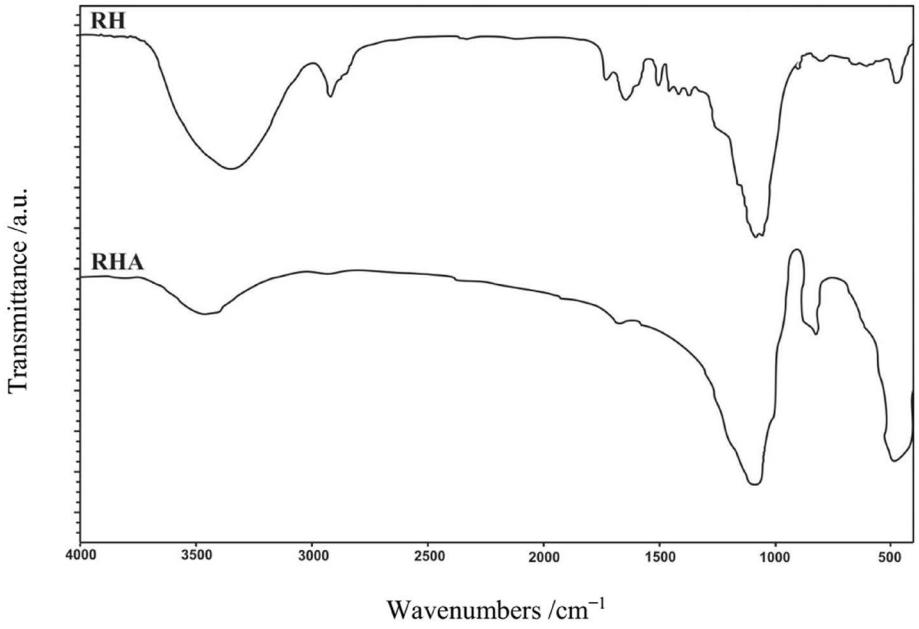

Fig. 3. FTIR of the RH and RHA.

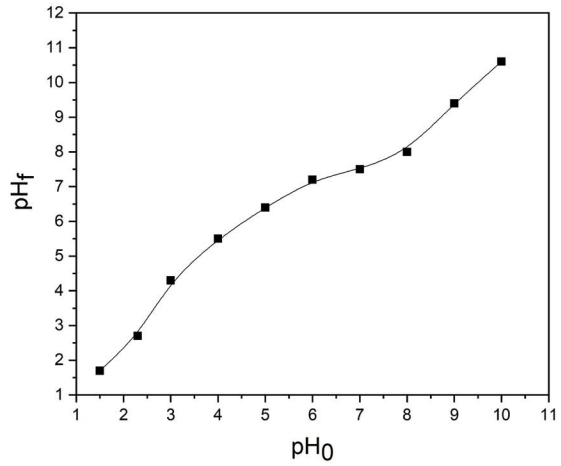

Fig. 4. Plot for determination of zero point charge for the RHS biosorbent.

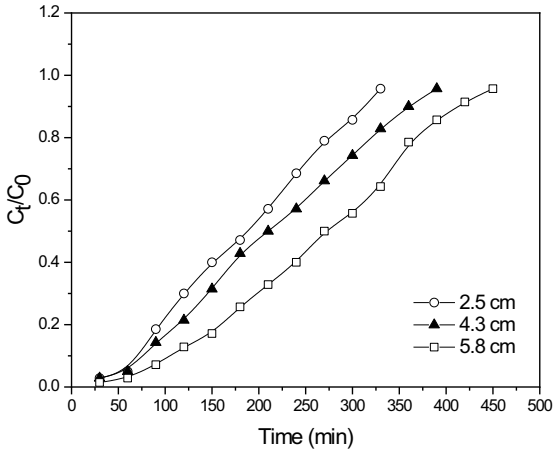

Fig. 5. Effect of various bed height on the breakthrough curve of Cr (VI) adsorption on RHA. Conditions: initial Cr (VI) concentration 100 mg/L; flow rate 5 mL/min; pH 2.5.

charge, causing repulsions and this outcome in the sorption reduction [36].

Many previous studies using pH 2.5 for maximum removal of Cr(VI) from aqueous solution. Because Cr(VI) ions can exist as hydrogen chromate ($HCrO^{4-}$) or dichromate ($Cr_2O_7^{2-}$) or chromate (CrO_4^{2-}) depending on the pH of the system [37].

At acidic pH 2.5, the dominant species form of Cr(VI) is $HCrO^{4-}$and as the pH increased other species forms $Cr_2O_7^{2-}$ or CrO_4^{2-} predominate. Observed higher adsorption at lower pH can be attributed to a large number of H^+ ions present at these pH values, which in turn neutralize the negatively charged hydroxyl group (–OH) on the adsorbed surface thereby reducing the hindrance to the diffusion of dichromate ions. Reduction in adsorption above pH 6 may be possible due to the abundance of OH^- ions causing increased hindrance to diffusion of $Cr_2O_7^{2-}$ ions [7,38].

3.2. Effect of different bed height

The performances of RHS biosorbent at various bed heights were investigated at a constant initial concentration of hexavalent chromium at 100 mg/L and rate of flow at 5 mL/min. As the bed height is raised, the total time (t_{total}) demanded also increased, which can be recognized from the plotted breakthrough curves in Fig. 5. Results confirmed that the total time and breakthrough time obviously relied on the height of the column bed. Fig. 5 demonstrates that reduced height of the column bed leads to faster bed saturation related to higher bed height. When bed height rises, hexavalent chromium percentage removal also raised from 60.6% to 89.3% as in Table 1. These results are due to more contact time for the interaction between RHS biosorbent and hexavalent chromium [39]. Table 1 shows that the biosorption capacity was not influenced remarkably with respect to the increase in height of the column bed.

3.3. Effect of flow rate

Three variable initial flow rates viz. 5, 10 and 15 mL/min were investigated to examine the RHS biosorbent performing at a constant initial concentration of hexavalent chromium, that is, 100 mg/L and a constant bed height of 4.3 cm. Diminution in breakthrough time as the rate of flow increased from 5 to 15 mL/min as shown in Fig. 6. Moreover, the total time (t_{total}) and biosorption capacity reduced with increased flow rate; results for which are illustrated in Table 1. Removal percentage (%) of hexavalent chromium reduced from 87.1% to 47.6% with an increased rate of flow. This reduction in RHS biosorption capacity was caused due to the lowered time of contact between RHS biosorbent and hexavalent chromium [40].

3.4. Effect of initial Cr (VI) concentration

In the adsorption of hexavalent chromium to RHS biosorbent, a change in inlet hexavalent chromium concentration influenced the performing characteristics of the fixed-bed column. The adsorption breakthrough curves attained by exchanging inlet hexavalent chromium concentration from

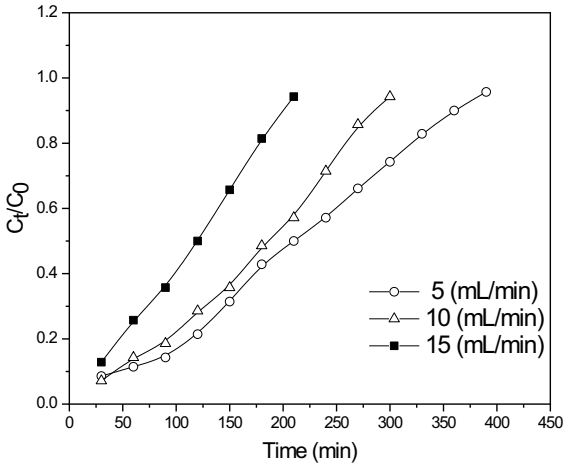

Fig. 6. Effect of various flow rates on the breakthrough curve of Cr (VI) adsorption on RHA. Conditions: bed height 4.3 cm; initial Cr (VI) concentration 100 mg/L; pH 2.5.

Table 1
Parameters in a fixed-bed column for Cr (VI) adsorption by RHA

C_0 (mg/ L)	Q (mL/min)	Z (cm)	pH	t_{total} (min)	V_{eff} (mL)	m_{total} (mg)	q_{total} (mg)	q_{eq} (mg/g)	Y%	D (g)
100	5	4.3	2.5	390	1,950	195	170	56.6	87.1	3
100	10	4.3	2.5	300	3,000	300	161	53.5	53.5	3
100	15	4.3	2.5	210	3,150	315	150	50	47.6	3
100	5	2.5	2.5	330	1,650	165	100	66.5	60.6	1.5
100	5	4.3	2.5	390	1,950	195	170	56.6	87.1	3
100	5	5.8	2.5	450	2,250	225	201	44.4	89.3	4.5
50	5	2.5	2.5	420	2,100	105	70	46.7	66.7	1.5
100	5	2.5	2.5	330	1,650	165	100	66.5	60.6	1.5
150	5	2.5	2.5	240	1,200	180	110	73.3	61	1.5

50 to 150 mg/L at 5 mL/min flow rate and 2.5 cm bed height are given in Fig. 6. The breakthrough time of the RHS biosorbent was decreased with an increasing initial hexavalent chromium concentration (Fig. 7). This could be explained by the fact that the driving force for adsorption is the hexavalent chromium concentration difference between the solution and the RHS biosorbent [41].

With the rise in the initial concentration of hexavalent chromium, total time (t_{total}), as well as RHS biosorption capacity, increased as shown in Table 1. Such results are due to the existence of hexavalent chromium molecules on the formed film layer which demonstrated quick transfer at higher concentrations to the biosorbent surface; since there was a raise in the coefficient of mass transfer [42]. Table 1 represents the removal percentage of hexavalent chromium reduced from 66.7% to 61% with the rise in initial hexavalent chromium concentration.

3.6. Breakthrough curve modeling

Successful column design for the adsorption process is the need for the breakthrough curve prediction for the effluent [26]. Several mathematical models have been applied in describing development and analysis of the lab-scale column reports for industrial applications [39]. Thomas, Yoon–Nelson and Adams–Bohart, models were used to develop the best model for expecting the dynamic performance of the column.

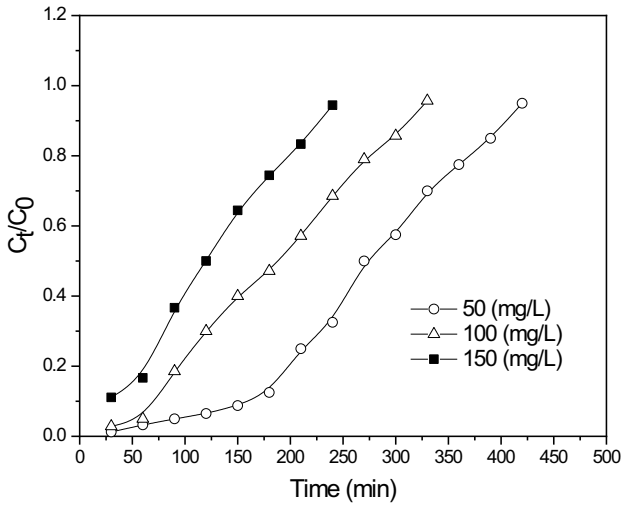

Fig. 7. Effect of initial Cr (VI) concentration on the breakthrough curve of Cr (VI) adsorption on RHA. Conditions: bed height 2.5 cm; flow rate 5 mL/min; pH 2.5.

3.6.1. Thomas model

One of the most general models is Thomas equation that is used in describing the interpretation of column data. This model assumed that adsorption equilibrium followed Langmuir-type isotherm and the adsorption process obeyed the pseudo-second-order reversible reaction kinetics. It also supposes when the limitations for diffusion of internal and external factors are absent [43].

Thomas model [44] infers plug flow performance in the column bed. It is widely used in describing the performance hypothesis of the sorption process in the column. The linear equation of this model is written as in the following expression:

$$\ln\left(\frac{C_0}{C_t}-1\right)=\frac{k_{Th}mq_{Th}^0}{Q}-k_{Th}C_0t \quad (6)$$

Here k_{Th} (the Thomas rate constant in mL/min mg), q_{Th}^0 (the maximum adsorption capacity of hexavalent chromium ions in mg/g), and t (the total flow time in min). Thomas model constants; k_{Th} and q_{Th}^0 are determined by graph drawn of $\ln[(C_0/C_t)-1]$ vs. time (t) (Fig. 8).

Linear regression analysis was employed to calculate correlation coefficient and relative constants according to Eq. (6) and Thomas model parameters are represented in Table 2. As seen from this table, the correlation regression coefficient which is a good fit with the experimental data (>0.97) suggests that the Thomas model well described the continuous biosorption of hexavalent chromium in the fixed-bed column of RHA. The k_{Th} values decreased with increasing bed height and initial hexavalent chromium ions concentration but increased with the increasing flow rate [45]. The values of q_{Th}^0 elevated with an increasing in both bed height and initial concentrations of hexavalent chromium ions but decreased with flow rate [19].

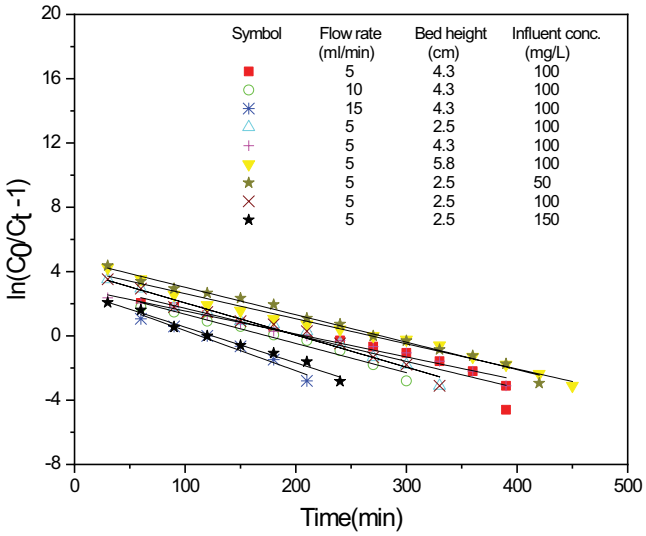

Fig. 8. Thomas model plots.

3.6.2. Yoon–Nelson model

Yoon–Nelson model was used in describing the adsorption system of the column. At lower or higher time intervals of the breakthrough curve, this model can be used in reducing the fault causing of Thomas model [46]. Yoon–Nelson [47] is a simple model established on sorption of gases on activated carbon. This model assumes that the probability of a reduction in adsorption capacity is proportional to the sorbate breakthrough achieved onto the sorbent surface [48]. Yoon–Nelson model linearized form is expressed by the following equation:

$$\ln\left(\frac{C_t}{C_0 - C_t}\right) = k_{YN}t - \tau k_{YN} \tag{7}$$

Here k_{YN} (the rate constant in min^{-1}) and τ (the time required for 50% sorbate in min). The values of k_{YN} and τ can be obtained from plotting of $\ln[C_t/(C_0–C_t)]$ vs. t (Fig. 9).

The values of the Yoon–Nelson model parameters were calculated and presented in Table 3, The Yoon–Nelson model plots were linear with high R^2 values (>0.94). This indicated that Yoon–Nelson model validity for biosorption of hexavalent chromium with RHA.

As shown in Table 3, the k_{YN} values elevated with an increase in both flow rate and initial concentration for hexavalent chromium adsorption. Whilst the 50% breakthrough time τ values are increased with increasing in bed height and decreased as the initial hexavalent chromium concentration increased. This due to column saturation occurring more quickly [26]. Both Thomas and Yoon–Nelson models have high values of R^2 that can be used to describe adsorption performance of packed column.

Consistent with the Yoon–Nelson model, the efficiency of the biosorption process can be computed as the amount of metal ion sorbed in a packed column is half of the total metal ion fed into the column during 2 τ period [49]. In this case, for a given bed, q^0_{YN} is the column sorption capacity in the Yoon–Nelson model that can be computed with the following equation:

$$q^0_{YN} = \frac{q_{total}}{M} = \frac{\left(\frac{1}{2}\right)C_0\left[\left(\frac{Q}{1{,}000}\right)\times 2\tau\right]}{M} = \frac{C_0 Q\,\tau}{1{,}000\times M} \tag{8}$$

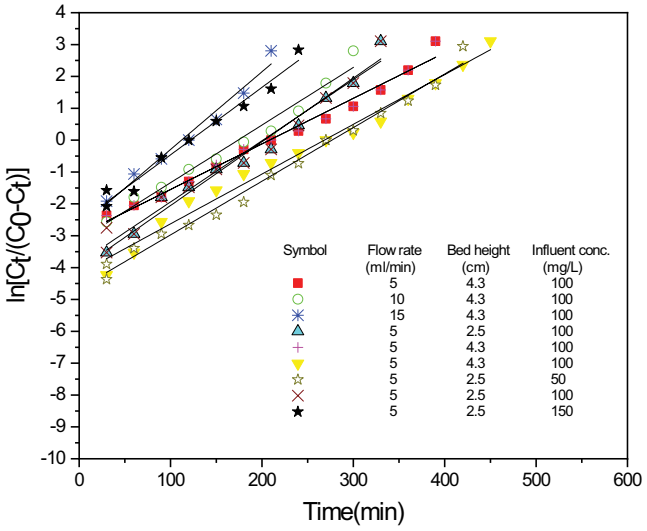

Fig. 9. Yoon–Nelson plots.

Table 2
Parameters of Thomas model under different conditions using linear regression analysis

C_0 (mg/L)	Q (mL/min)	Z (cm)	pH	k_{Th} (mL/mg min)	q^0_{Th} (mg/g)	R^2
100	5	4.3	2.5	0.000143	50.69	0.984
100	10	4.3	2.5	0.0001808	85.73	0.972
100	15	4.3	2.5	0.0002437	88.94	0.970
100	5	2.5	2.5	0.0001999	100.05	0.973
100	5	4.3	2.5	0.000143	50.69	0.984
100	5	5.8	2.5	0.00014061	48.59	0.981
50	5	2.5	2.5	0.0003416	68.79	0.988
100	5	2.5	2.5	0.0001999	100.05	0.973
150	5	2.5	2.5	0.0001479	104.77	0.988

Table 3
Parameters of Yoon–Nelson model under different conditions using linear regression analysis

C_0 (mg/L)	Q (mL/min)	Z (cm)	pH	k_{YN} (min^{-1})	τ min	t_{exp} min	q^0_{YN} (mg/g)	R^2
100	5	4.3	2.5	0.0142	232.39	210	58.09	0.982
100	10	4.3	2.5	0.01805	113.57	180	56.78	0.962
100	15	4.3	2.5	0.02654	71.59	120	53.69	0.973
100	5	2.5	2.5	0.01955	148.33	180	74.16	0.971
100	5	4.3	2.5	0.0142	232.39	210	58.09	0.982
100	5	5.8	2.5	0.014051	270.44	270	45.07	0.977
50	5	2.5	2.5	0.01703	211.39	260	52.84	0.985
100	5	2.5	2.5	0.01955	148.33	210	74.16	0.970
150	5	2.5	2.5	0.022	109.09	120	81.81	0.973

Here C_0 (the initial concentration of hexavalent chromium ions in mg/L), Q (flow rate in mL/min), M (the weight of sorbent in g) and τ (the time required for 50% sorbate breakthrough). The values of q^0_{YN} elevated with increasing bed height and initial concentrations of hexavalent chromium ions but decreased with flow rate [50].

3.6.3. Adams–Bohart model

Adams and Bohart [51] using surface hypothesis explained a fundamental equation and it describes a dynamic relationship between C_t/C_0 and t in a packed column. It supposes that adsorption equilibrium is not an instant phenomenon. It is often applied to describe the initial part of the obtained breakthrough curve. Adams and Bohart model linearized form is expressed using the following equation:

$$\ln\frac{C_t}{C_0} = k_{AB}C_0 t - k_{AB}N_0\left(\frac{Z}{U_0}\right) \tag{9}$$

Here C_0 (initial hexavalent chromium concentration), C_t (effluent hexavalent chromium concentration at selected time t in mg/L), k_{AB} (Adams–Bohart kinetic constant in L/mg min), N_0 (the saturation concentration in mg/L), Z (the bed height of the fixed-bed column in cm), U_0 (the linear velocity in cm/min). The time is taken in the range of the breakthrough curve from the beginning to the end. The values of k_{AB} and N_0 are obtained from plotting of ln (C_t/C_0) vs. t (Fig. 10).

Linear regression analysis was used for computing k_{AB} and N_0 values, which is presented in Table 4. The correlation coefficients values of Thomas model ranging from 0.97 to 0.98 provided a better fit of the data comparing with Adams–Bohart model. It is observed from Table 4 that the values of k_{AB} reduced with increasing initial hexavalent chromium concentrations and flow rates but elevated with an increasing bed heights. It was indicated that the overall process kinetics was controlled by external mass transfer during the initial part of the sorption process in the column [52]. This model provides thorough and simple approach to run and evaluate the biosorption of hexavalent chromium ion in RHA-packed column; nevertheless, its validity is limited in the range of conditions used [30].

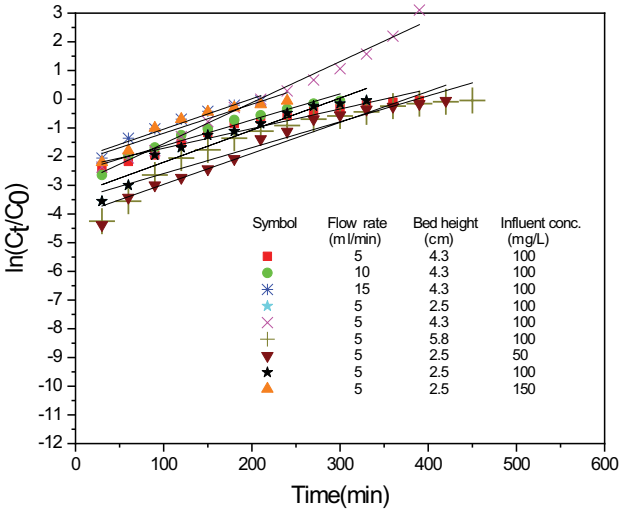

Fig. 10. Adams–Bohart plots.

The Thomas, Yoon–Nelson, and Adams–Bohart models were used to predict the breakthrough curves of the biosorption process (Fig. 11). At all experimental conditions, the predicted curves proposed by Yoon–Nelson model were in sensibly better agreement with the empirical curves than the Thomas and Adams–Bohart models.

It is observed that breakthrough curves at the lower and high time, the fitted curves of the Adams–Bohart model were far away from experimental data. Therefore, the Yoon–Nelson model was appeared to agree to predict the hexavalent chromium ions column biosorption better than the Thomas and Adams–Bohart models. The q^0_{YN} values are closer for q_{eq} values in Table 1 than q^0_{Th} values and values of τ can be compared with values of t experiments in Table 3 which indicated that the Yoon–Nelson model can describe the column kinetics more than Thomas and Adams–Bohart models which corresponds to several scientists studied the removal of metal by biosorption in the packed column [53,54].

4. Conclusion

The RHA was used for the biosorption of hexavalent chromium ions from aqueous solution by fixed-bed column.

Table 4
Parameters of Adams–Bohart model under different conditions using linear regression analysis

C_0 (mg/L)	Q (mL/min)	Z (cm)	pH	N_0 (mg/L)	k_{AB} (L/mg min)	R^2
100	5	4.3	2.5	25,926.6	0.0000684	0.925
100	10	4.3	2.5	40,904.1	0.0000907	0.946
100	15	4.3	2.5	44,141.7	0.0001059	0.936
100	5	2.5	2.5	37,704.5	0.0001117	0.908
100	5	4.3	2.5	25,926.6	0.0000684	0.925
100	5	5.8	2.5	20,712.6	0.0000903	0.859
50	5	2.5	2.5	47,312	0.0001079	0.94
100	5	2.5	2.5	37,704.5	0.0001117	0.908
150	5	2.5	2.5	26,588.3	0.0001008	0.875

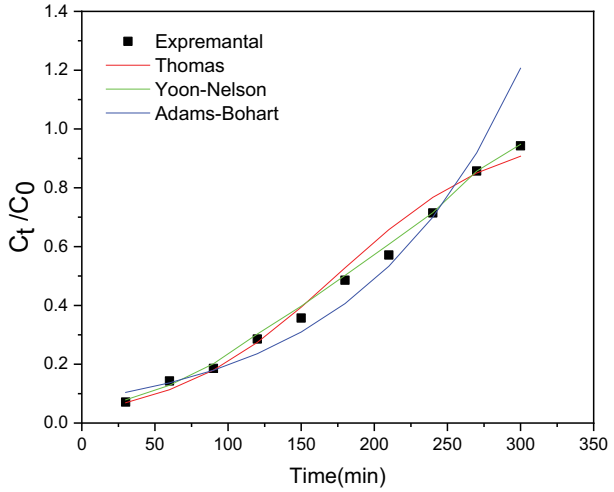

Fig. 11. Experimental and predicted breakthrough curves using the Thomas, Yoon–Nelson, and Adams–Bohart models for the sorption of Cr (VI) by RHA at an inlet hexavalent chromium concentration of 100 mg/L, flow rate 10 mL/min and bed height 4.3 cm.

Hexavalent chromium ions uptake carried out by a fixed-bed column was seemed to be dependent on the bed height, initial hexavalent chromium ions concentration, and flow rate. The biosorption capacity was elevated with an increasing in bed height but reduced with increasing initial concentration and flow rate. The performance of the column process was achieved better at larger bed height, lower flow rate and lower initial hexavalent chromium ions concentration. Thomas, Yoon–Nelson, and Adams–Bohart mathematical models were successfully used to predict the experimental breakthrough curves. Yoon–Nelson model was found suitable for describing of RHA breakthrough curves than Thomas model under various column conditions. It is considered an economy technique for removal of hexavalent chromium ions in manufacturing effluent management technique.

Acknowledgment

This work was supported by Researchers Supporting Project number (RSP-2019/100), King Saud University, Riyadh, Saudi Arabia.

References

[1] M. Naushad, T. Ahamad, B.M. Al-Maswari, A. Abdullah Alqadami, S.M. Alshehri, Nickel ferrite bearing nitrogen-doped mesoporous carbon as efficient adsorbent for the removal of highly toxic metal ion from aqueous medium, Chem. Eng. J., 330 (2017) 1351–1360.
[2] M.M. El-Sheekh, A.A. Farghl, H.R. Galal, H.S. Bayoumi, Bioremediation of different types of polluted water using microalgae, Rend. Lincei Sci. Fis. Nat., 27 (2016) 401–410.
[3] M.K. Sabullah, M.R. Sulaiman, M.S. Shukor, M.T. Yusof, W.L.W. Johari, M.Y. Shukor, A. Syahir, Heavy metals biomonitoring via inhibitive assay of acetylcholinesterase from *Periophthalmodon schlosseri*, Rend. Lincei Sci. Fis. Nat., 26 (2015) 151–158.
[4] M. Sohail, M.N. Khan, A.S. Chaudhry, N.A. Qureshi, Bioaccumulation of heavy metals and analysis of mineral element alongside proximate composition in foot, gills and mantle of freshwater mussels (*Anodonta anatina*), Rend. Lincei Sci. Fis. Nat., 27 (2016) 687–696.
[5] Z. Aksu, F. Gönen, Biosorption of phenol by immobilized activated sludge in a continuous packed bed: prediction of breakthrough curves, Process Biochem., 39 (2004) 599–613.
[6] E. Malkoc, Y. Nuhoglu, M. Dundar, Adsorption of chromium (VI) on pomacan olive oil industry waste: batch and column studies, J. Hazard. Mater., 138 (2006) 142–151.
[7] V.K. Gupta, A. Rastogi, A. Nayak, Adsorption studies on the removal of hexavalent chromium from aqueous solution using a low cost fertilizer industry waste material, J. Colloid Interface Sci., 342 (2010) 135–141.
[8] Y.A. Aydın, N.D. Aksoy, Adsorption of chromium on chitosan: Optimization, kinetics and thermodynamics, Chem. Eng. J., 151 (2009) 188–194.
[9] M. Habuda-Stanić, M.E. Ravančić, A. Flanagan, A review on adsorption of fluoride from aqueous solution, Materials, 7 (2014) 6317–6366.
[10] Z. Harrache, M. Abbas, T. Aksil, M. Trari, Thermodynamic and kinetics studies on adsorption of Indigo Carmine from aqueous solution by activated carbon, Microchem. J., 144 (2019) 180–189.
[11] P.A. Kumar, S. Chakraborty, Fixed-bed column study for hexavalent chromium removal and recovery by short-chain polyaniline synthesized on jute fiber, J. Hazard. Mater., 162 (2009) 1086–1098.
[12] V.C. Srivastava, I.D. Mall, I.M. Mishra, Adsorption thermodynamics and isosteric heat of adsorption of toxic metal ions onto bagasse fly ash (BFA) and rice husk ash (RHA), Chem. Eng. J., 132 (2007) 267–278.
[13] R. Pode, Potential applications of rice husk ash waste from rice husk biomass power plant, Renew. Sust. Energy Rev., 53 (2016) 1468–1485.
[14] J. Prasara-A, S.H. Gheewala, Sustainable utilization of rice husk ash from power plants: a review, J. Clean. Prod., 167 (2017) 1020–1028.

[15] P. Sharma, R. Kaur, C. Baskar, W.-J. Chung, Removal of methylene blue from aqueous waste using rice husk and rice husk ash, Desalination, 259 (2010) 249–257.
[16] U.R. Lakshmi, V.C. Srivastava, I.D. Mall, D.H. Lataye, Rice husk ash as an effective adsorbent: evaluation of adsorptive characteristics for Indigo Carmine dye, J. Environ. Manage., 90 (2009) 710–720.
[17] F. Adam, J.-H. Chua, The adsorption of palmytic acid on rice husk ash chemically modified with Al(III) ion using the sol–gel technique, J. Colloid Interface Sci., 280 (2004) 55–61.
[18] A. Imagawa, R. Seto, Y. Nagaosa, Adsorption of chlorinated hydrocarbons from air and aqueous solutions by carbonized rice husk, Carbon, 4 (2000) 623–641.
[19] E. Nakkeeran, C. Patra, T. Shahnaz, S. Rangabhashiyam, N. Selvaraju, Continuous biosorption assessment for the removal of hexavalent chromium from aqueous solutions using *Strychnos nux vomica* fruit shell, Bioresour. Technol. Rep., 3 (2018) 256–260.
[20] N. Saranya, A. Ajmani, V. Sivasubramanian, N. Selvaraju, Hexavalent chromium removal from simulated and real effluents using *Artocarpus heterophyllus* peel biosorbent - batch and continuous studies, J. Mol. Liq., 265 (2018) 779–790.
[21] S. Rangabhashiyam, E. Suganya, N. Selvaraju, Packed bed column investigation on hexavalent chromium adsorption using activated carbon prepared from *Swietenia mahogani* fruit shells AU -, Desal. Wat. Treat., 57 (2016) 13048–13055.
[22] A.K. Bhattacharya, T.K. Naiya, S.N. Mandal, S.K. Das, Adsorption, kinetics and equilibrium studies on removal of Cr(VI) from aqueous solutions using different low-cost adsorbents, Chem. Eng. J., 137 (2008) 529–541.
[23] R. Kumar, D. Bhatia, R. Singh, S. Rani, N.R. Bishnoi, Sorption of heavy metals from electroplating effluent using immobilized biomass *Trichoderma viride* in a continuous packed-bed column, Int. Biodeterior. Biodegrad., 65 (2011) 1133–1139.
[24] S. Banerjee, S.R. Joshi, T. Mandal, G. Halder, Application of zirconium caged activated biochar alginate beads towards deionization of Cr(VI) laden water in a fixed bed column reactor, J. Environ. Chem. Eng., 6 (2018) 4018–4029.
[25] N.H. Mthombeni, S. Mbakop, S.C. Ray, T. Leswifi, A. Ochieng, M.S. Onyango, Highly efficient removal of chromium (VI) through adsorption and reduction: a column dynamic study using magnetized natural zeolite-polypyrrole composite, J. Environ. Chem. Eng., 6 (2018) 4008–4017.
[26] A.P. Lim, A.Z. Aris, Continuous fixed-bed column study and adsorption modeling: removal of cadmium (II) and lead (II) ions in aqueous solution by dead calcareous skeletons, Biochem. Eng. J., 87 (2014) 50–61.
[27] Q.-Q. Zhong, X. Xu, L. Shen, Y.-J. Han, Y.-C. Hao, Breakthrough curve analysis of *Enteromorpha prolifera* packed fixed-bed column for the biosorption, Environ. Eng. Sci., 35 (2018) 864–874.
[28] N. Chen, Z. Zhang, C. Feng, M. Li, R. Chen, N. Sugiura, Investigations on the batch and fixed-bed column performance of fluoride adsorption by Kanuma mud, Desalination, 268 (2011) 76–82.
[29] Y. Zhang, L. Xiong, Y. Xiu, K. Huang, Defluoridation in fixed bed column filled with Zr(IV)-loaded garlic peel, Microchem. J., 145 (2019) 476–485.
[30] R. Han, L. Zou, X. Zhao, Y. Xu, F. Xu, Y. Li, Y. Wang, Characterization and properties of iron oxide-coated zeolite as adsorbent for removal of copper (II) from solution in fixed bed column, Chem. Eng. J., 149 (2009) 123–131.
[31] E. Oguz, M. Ersoy, Removal of Cu^{2+} from aqueous solution by adsorption in a fixed bed column and neural network modelling, Chem. Eng J., 164 (2010) 56–62.
[32] M. Abbas, S. Kaddour, M. Trari, Kinetic and equilibrium studies of cobalt adsorption on apricot stone activated carbon, J. Ind. Eng. Chem., 20 (2014) 745–751.
[33] S.F. Montanher, E.A. Oliveira, M.C. Rollemberg, Removal of metal ions from aqueous solutions by sorption onto rice bran, J. Hazard. Mater., 117 (2005) 207–211.
[34] S. Genieva, S. Turmanova, A. Dimitrova, L. Vlaev, Characterization of rice husks and the products of its thermal degradation in air or nitrogen atmosphere, J. Therm. Anal. Calorim., 93 (2008) 387–396.
[35] S. Chandrasekhar, P.N. Pramada, Rice husk ash as an adsorbent for methylene blue—effect of ashing temperature, Adsorption, 12 (2006) 27.
[36] S. Ravulapalli, R. Kunta, Enhanced removal of chromium (VI) from wastewater using active carbon derived from *Lantana camara* plant as adsorbent, Water Sci. Technol., 78 (2018) 1377–1389.
[37] S. Rangabhashiyam, N. Selvaraju, Adsorptive remediation of hexavalent chromium from synthetic wastewater by a natural and $ZnCl_2$ activated *Sterculia guttata* shell, J. Mol. Liq., 207 (2015) 39–49.
[38] V.E. Pakade, O.B. Nchoe, L. Hlungwane, N.T. Tavengwa, Sequestration of hexavalent chromium from aqueous solutions by activated carbon derived from Macadamia nutshells, Water Sci. Technol., 75 (2016) 196–206.
[39] V. Vinodhini, N. Das, Packed bed column studies on Cr (VI) removal from tannery wastewater by neem sawdust, Desalination, 264 (2010) 9–14.
[40] D. Bulgariu, L. Bulgariu, Sorption of Pb(II) onto a mixture of algae waste biomass and anion exchanger resin in a packed-bed column, Bioresour. Technol., 129 (2013) 374–380.
[41] C. Quintelas, B. Fernandes, J. Castro, H. Figueiredo, T. Tavares, Biosorption of Cr(VI) by a *Bacillus coagulans* biofilm supported on granular activated carbon (GAC), Chem. Eng. J., 136 (2008) 195–203.
[42] J. Samuel, M. Pulimi, M.L. Paul, A. Maurya, N. Chandrasekaran, A. Mukherjee, Batch and continuous flow studies of adsorptive removal of Cr(VI) by adapted bacterial consortia immobilized in alginate beads, Bioresour. Technol., 128 (2013) 423–430.
[43] Y.A. Mustafa, M.J. Zaiter, Treatment of radioactive liquid waste (Co-60) by sorption on Zeolite Na-A prepared from Iraqi kaolin, J. Hazard. Mater., 196 (2011) 228–233.
[44] H.C. Thomas, Heterogeneous ion exchange in a flowing system, J. Am. Chem. Soc., 66 (1944) 1664–1666.
[45] H. Karunarathne, B. Amarasinghe, Fixed bed adsorption column studies for the removal of aqueous phenol from activated carbon prepared from sugarcane bagasse, Energy Procedia, 34 (2013) 83–90.
[46] R. Sharma, B. Singh, Removal of Ni (II) ions from aqueous solutions using modified rice straw in a fixed bed column, Bioresour. Technol., 146 (2013) 519–524.
[47] Y.H. Yoon, J.H. Nelson, Application of gas adsorption kinetics I. A theoretical model for respirator cartridge service life, Am. Ind. Hyg. Assoc. J., 45 (1984) 509–516.
[48] M. Calero, F. Hernáinz, G. Blázquez, G. Tenorio, M. Martín-Lara, Study of Cr (III) biosorption in a fixed-bed column, J. Hazard. Mater., 171 (2009) 886–893.
[49] İ.Y. İpek, N. Kabay, M. Yüksel, Modeling of fixed bed column studies for removal of boron from geothermal water by selective chelating ion exchange resins, Desalination, 310 (2013) 151–157.
[50] W. Zou, L. Zhao, Removal of uranium(VI) from aqueous solution using citric acid modified pine sawdust: batch and column studies, J. Radioanal. Nucl. Chem., 292 (2011) 585–595.
[51] G. Bohart, E. Adams, Some aspects of the behavior of charcoal with respect to chlorine, J. Am. Chem. Soc., 42 (1920) 523–544.
[52] A. Ahmad, B. Hameed, Fixed-bed adsorption of reactive azo dye onto granular activated carbon prepared from waste, J. Hazard. Mater., 175 (2010) 298–303.
[53] M.A.E. de Franco, C.B. de Carvalho, M.M. Bonetto, R. de Pelegrini Soares, L.A. Féris, Diclofenac removal from water by adsorption using activated carbon in batch mode and fixed-bed column: isotherms, thermodynamic study and breakthrough curves modeling, J. Clean. Prod., 181 (2018) 145–154.
[54] H.E. Reynel-Avila, D.I. Mendoza-Castillo, A. Bonilla-Petriciolet, J. Silvestre-Albero, Assessment of naproxen adsorption on bone char in aqueous solutions using batch and fixed-bed processes, J. Mol. Liq., 209 (2015) 187–195.